

Interfacial Tension Measurements of the (H₂O + *n*-Decane + CO₂) Ternary System at Elevated Pressures and Temperatures

Apostolos Georgiadis, Geoffrey Maitland, J. P. Martin Trusler, and Alexander Bismarck*

Department of Chemical Engineering and Chemical Technology, Imperial College London, London SW7 2AZ, United Kingdom

ABSTRACT: The interfacial tension between H₂O and [(1 - *x*)*n*-decane + *x*CO₂] was investigated for three different compositions of CO₂ in the alkane-rich phase, of mole fractions *x* = (0.0, 0.2, and 0.5), along several isotherms at temperatures up to 443 K and pressures ranging from the miscibility state points for (*n*-decane + CO₂) up to 50 MPa. The pendant drop method was implemented using a high pressure apparatus consisting of a view cell, fitted with a high pressure capillary tube for creating pendant H₂O drops in the [*n*-decane + CO₂] bulk phase. The conditions investigated cover a wide range relevant to carbon storage, providing information as to how the variation of the CO₂ content in hydrocarbon fluids affects their interfacial tension with aqueous phases, which influences the trapping potential of underground formations. The results were compared to literature values where possible. A thermodynamic analysis of the dependence of the interfacial tension on CO₂ composition, as well as on temperature, was discussed with respect to the Gibbs surface excess concentration and the enthalpy of interface formation, respectively. The present work provides novel interfacial tension data for the ternary system and addresses possible reasons for the observed discrepancies in literature values for the binary (H₂O + *n*-decane) system observed over the range of conditions investigated. The reported results have a relative average standard deviation of 1.7 %.

INTRODUCTION

The mitigation of climate change through carbon capture and storage (CCS), combined with the use of CO₂ as an enhanced reservoir process fluid, is a promising scheme for the transition period from global energy reliance on hydrocarbon sources to more sustainable operations. A detailed account of the relevant processes involved and storage in porous rocks by capillary forces has been given previously.^{1,2} The main cause of capillary trapping is ultimately linked to the interfacial properties of CO₂ with the existing fluids in the reservoir—mainly aqueous and hydrocarbon phases. The interfacial tension, γ , of mixtures representative of the fluids in underground formations in the presence of CO₂ is an important thermophysical property for the design of such processes.

The interfacial tension of the (H₂O + CO₂)¹ and various (*n*-alkane + CO₂) systems² has been investigated by the authors recently. The present work has focused on the interfacial tension of those systems combined, investigating the (H₂O + [*n*-alkane + CO₂]) ternary mixture—a relevant property for CO₂ sequestration in depleted oil reservoirs, as all three components are likely to be present in such formations.^{3,4} A number of contributions have focused on measurements of binary (aqueous + hydrocarbon) systems;^{5–13} however, no literature sources were found to have studied ternary systems with CO₂ present as a third component.

Essential to the characterization of interfacial properties is the temporal dependence that each system may exhibit. The time dependence of the interfacial tension for (H₂O + *n*-alkane) systems is more pronounced than that observed previously for the (H₂O + CO₂)¹ or (*n*-alkane + CO₂) systems,² which is expected as impurities tend to migrate strongly to (aqueous + hydrocarbon) interfaces. Hence, purification of the *n*-alkane phases prior to measurement is very important as the hydrocarbon

itself can oxidize with time, or oxidized forms may remain from distillation processes involved in producing the compound, which then act as surfactants in an (aqueous + hydrocarbon) interface. This is an observation made by a number of authors, and usually purification of the *n*-alkane requires the use of a column with activated alumina, through which the fluid is passed several times so that oxidized alkanes (R–O, R–OH, R–OOH) are removed by adsorbing onto the activated particles.^{12–17} In fact, Goebel and Lunkenheimer¹² and Horozov et al.¹⁴ report the time dependence of the interfacial tension measured prior to and after purification for (aqueous + hydrocarbon) systems and show that no time dependence should be expected for the purified fluids. Table 1 summarizes the literature values and purification procedures followed for the (H₂O + *n*-decane) system by different authors in comparison with the present work. It can be seen that there is considerable scatter in the data of the order >10%.

At elevated temperatures and pressures, interfacial tension measurements are more limited and more prone to effects from the presence of trace amounts of impurities due to the inherent increased complexity of the appropriate measuring equipment. Michaels and Hauser⁵ (1951) seem to be of the first to have experimentally measured interfacial tensions of H₂O and alkanes at pressures up to 70 MPa and temperatures up to 303 K, using the pendant drop method. They worked with the systems (H₂O + benzene) and (H₂O + *n*-decane) using the tables of Andreas et al.¹⁸ to compute and plot the interfacial

Special Issue: Kenneth N. Marsh Festschrift

Received: July 29, 2011

Accepted: August 23, 2011

Published: October 04, 2011

Table 1. Literature Values of Interfacial Tension for the (H₂O + *n*-Decane) System^a

| authors et al. | year | method | purification | dγ/dt | γ | T |
|------------------------|------|--------|--------------|--------|--------------------------------|-------|
| | | | | | mN · m ⁻¹ | K |
| Michaels ⁵ | 1951 | PD-SP | FC | | 46.5 | 296 |
| Aveyard ¹⁵ | 1965 | DV | AC | stable | 52.3 | 293 |
| Jennings ⁷ | 1967 | PD-SP | FC | | 51.2 | 298 |
| Susnar ¹⁰ | 1994 | PD-DSA | NO | <0 | 51.59 (<i>t</i> = 0) | 295.6 |
| Wiegand ⁹ | 1994 | PD-SP | | | 51.10 | 295 |
| Cai ¹¹ | 1996 | PD-DSA | NO | | 51.55 | 298 |
| Goebel ¹² | 1997 | PD-SP | AC | stable | 53.2 | 295 |
| Zeppieri ¹³ | 2001 | PD-DSA | AC | stable | 52.33 | 293 |
| present work | 2011 | PD-DSA | AC | stable | 51.96 (60 < <i>t</i> /s < 180) | 297.9 |

^a Measured using: DV = drop volume, PD = pendant drop, DSA = drop shape analysis, SP = selected plane. Purification methods followed were either by fractionation (FC) or using an alumina column (AC).

tension to gravitational force ratio, $\gamma/\Delta\rho g$, as a function of temperature and pressure. They then used the density difference of the pure compounds to calculate the interfacial tension, commenting that this assumption should introduce an error up to 2 % due to discrepancies in the literature values at the time of *n*-decane densities at elevated temperatures. An important observation made by Michaels and Hauser⁵ was the dependence of the interfacial tension on effective cleaning procedures followed for the removal of trace amounts of impurities present in a high pressure apparatus. By comparing the values obtained at ambient pressure with independent measurements carried out in a different all-glass and thoroughly cleaned equipment, they found a 2 % deviation in the interfacial tension of the (H₂O + *n*-decane) system, which they attribute to less effective removal of impurities from a high pressure apparatus.

Jennings⁷ also conducted measurements for the systems (H₂O + benzene) and (H₂O + *n*-decane), using the pendant drop selected plane method, at pressures up to 80 MPa and temperatures up to 450 K. These measurements gave higher interfacial tensions than reported by Michaels and Hauser,⁵ attributed by the author to the use of better purification and cleaning procedures. Jennings and Newman⁸ also measured interfacial tensions of the (H₂O + methane + *n*-decane) system for the whole range of methane mole fractions over the same range of conditions.

In 1994, Wiegand and Franck⁹ measured the interfacial tension of several alkanes with H₂O at high pressures up to 300 MPa and temperatures up to 473 K. They also used the pendant drop selected plane method of Andreas et al.¹⁸ and considered the densities of the two phases to be those of the pure compounds. Susnar et al.¹⁰ investigated the (H₂O + *n*-decane) system at pressures up to 36 MPa and at ambient temperature using the axisymmetric drop shape analysis (ADSA) method.¹⁹ This appears to be the first time that the selected plane method of Andreas et al.¹⁸ was not used. Susnar et al.¹⁰ also stated that the density dependence resulting from the diffusion of one phase into the other is negligible, and therefore, it was also assumed that the densities of the two phases were those of the pure compounds. Susnar et al.¹⁰ focused on determining the effects of minor impurities on the interfacial tension, mentioning detailed cleaning procedures for avoiding surface active agents being present in the system. The conclusion was that it is impossible to be completely sure that no impurities exist in the system and, therefore, the values taken immediately after the drop's formation

should be more reliable. However, this is true only if the two fluids have previously been saturated with the other component, as was done in their experiments. The dependence of interfacial tension on pressure for these systems showed a small linear increase, consistent with previous researchers. The results of Susnar et al.¹⁰ agree with those of Wiegand and Franck,⁹ while both give values almost 10 % higher than Michael et al. for the (H₂O + *n*-decane) system.

Cai et al.¹¹ (1996) studied the interfacial tension of H₂O with different hydrocarbons at (298 and 323) K over a pressure range up to 30 MPa using the pendant drop method as well. Bahramian et al.²⁰ (2007) measured the interfacial tension of the ternary (H₂O + *n*-decane + methane) and the quaternary (H₂O + cyclohexane + *n*-decane + methane) systems at pressures up to 28 MPa at 423 K using the pendant drop method. For the phase density determination, they used a removable high pressure cell of known volume, and by measuring the weight each time, they were able to derive the density difference, $\Delta\rho$.

EXPERIMENTAL SECTION

Materials. The CO₂ used was of CP grade, supplied by BOC in a cylinder fitted with a dip tube for liquid withdrawal, of mole fraction purity >0.9995. The H₂O used was deionized, supplied by an ELGA Purelab Option-R water purifier, which has specifications better than those of double-distilled H₂O (water conductivity <15 $\mu\text{S} \cdot \text{cm}^{-1}$). The Purelab Option-R applies pretreatment, reverse osmosis, ion exchange, photo-oxidation, and recirculation as purification processes. Hexane (BDH, Hull, U.K.), isopropanol (Sigma-Aldrich, Dorset, U.K.), and toluene (Sigma-Aldrich, Dorset, U.K.), used for cleaning purposes, were of mole fraction purities >0.95, 0.999, and 0.999, respectively. The *n*-decane used for the interfacial tension measurements was of mole fraction purity >0.990. Additional purification treatment was applied; the *n*-decane was passed in a sequence of three steps through activated alumina, neutral (Sigma-Aldrich, Dorset, UK) for adsorbing oxidized forms of the alkane that act as surfactants in an (aqueous + hydrocarbon) system.

High-Pressure Apparatus and Procedure. A custom-designed high-pressure view cell of 24 cm³ inner volume was used to conduct interfacial tension measurements at elevated pressures and temperatures. The apparatus (Eurotechnica GmbH, model PD-E700 LL, Bargteheide, Germany), which has been described in detail previously,¹ was designed to hold pressures up

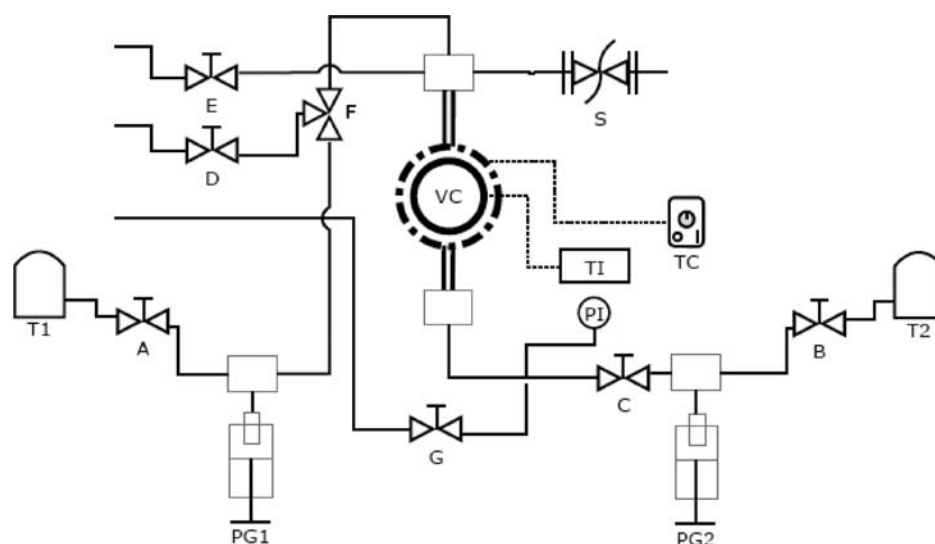


Figure 1. Flow diagram of the PD-E700 LL apparatus. In the diagram the following are annotated: view-cell (VC); pressure transducer (PI); thermocouple (TI); temperature controller (TC); pressure generators (PG1 and PG2); liquid supply tanks (T1 and T2); valves (A to E); valve connecting with gas supply (G); and safety rupture disk (S). The dash–dotted line around the view cell indicates a heating jacket, and the double lines connecting to the view cell indicate a 6.4 mm outer diameter (o.d.) high pressure tubing through which 1.6 mm o.d. capillary tubes reach into the view cell.

to 70 MPa at temperatures up to 473 K. A schematic diagram of the apparatus is shown in Figure 1.

The apparatus was thoroughly cleaned before use with appropriate solvents such as hexane, isopropanol, and/or toluene to dissolve any compounds remaining from previously conducted experiments. It was then drained, flushed with CO₂, and subsequently put under vacuum at a temperature of 323 K. This ensured that any remaining solvent was completely evaporated. All glassware was cleaned in concentrated KOH-isopropanol solution and was repeatedly rinsed with deionized H₂O before use. This ensured that no oil impurities would dissolve in the H₂O phase during handling.

The view cell was filled with a known quantity (measured with a glass pipet) of *n*-decane using the right-hand pressure generator “PG2” (see apparatus flow diagram in Figure 1). This amount was enough for filling completely the view cell and relevant tubings until the separating valve “F”, allowing at the same time for some additional amount in the pressure generator for using to raise the pressure further. The left-hand pressure generator “PG1” was completely filled with H₂O, which was isolated from the *n*-decane filled view cell by valve “F”. The latter was thereafter opened only for allowing a H₂O drop to be created within the view cell and was immediately closed, isolating the unsaturated H₂O phase from the *n*-decane-rich phase. CO₂ was introduced into the system via the high pressure syringe pump connected to valve “G”, only for the purpose of increasing the CO₂ mole fraction in the *n*-decane-rich phase, and was immediately closed when the appropriate amount was introduced. The syringe pump maintained the CO₂ at a pressure of 10 MPa, in the liquid state, and by monitoring the change of the volume in the pump when displacing CO₂ into the system, the mass introduced was calculated by multiplying with its density, at these conditions. The CO₂ was introduced at ambient temperature, being initially visible as it bubbled up through the *n*-decane and accumulated at the top of the view cell. By further compressing the system above the miscibility point, using the right-hand pressure generator, the gas phase dissolved into the liquid phase, bringing the three-component

system into the biphasic state. The system was allowed to equilibrate, usually by leaving overnight, prior to commencing with creating H₂O pendant drops in the [*n*-decane + CO₂] phase for measuring the interfacial tension. The uncertainty of the displayed volume of the syringe pump was ± 0.05 mL; taking into account environmental effects, however, the procedure was checked prior to the experiment by injecting CO₂ directly into the evacuated view cell of fixed volume several times, obtaining an average value of its volume with a standard deviation of ± 0.1 mL. The latter, at the conditions of CO₂ addition, corresponds to an uncertainty in the amount added of ± 0.19 mol, which relative to the CO₂ amounts measured in the present systems leads to an uncertainty in composition of $u(x) = 0.025$.

For every state point, four consecutive drops were created, each monitored for at least 900 s. The drop shape analysis software (Krüss GmbH, DSA V1.90.0.14, Hamburg, Germany) was set to capture frames every 4 s, which were all later analyzed for the calculation of the interfacial tension. The equation that relates the interfacial tension, γ , with the shape of a pendant drop can be given in the form

$$\gamma = \frac{\Delta\rho g}{(Bk_{\text{apex}})^2} \quad (1)$$

where $\Delta\rho$ is the density difference between the two phases, $g = 9.81 \text{ m} \cdot \text{s}^{-2}$ is the local gravitational acceleration, B is the shape parameter determined from the profile of a pendant drop, and k_{apex} is the curvature at the drop's apex. A detailed description of the drop shape analysis method has been given previously.¹

After the creation of every drop, the analysis of each captured frame revealed an initial transition period during which the interfacial tension dropped rapidly, similar to observations for the (H₂O + CO₂) system studied previously.¹ A stable value for the present system, however, was not as straightforward to achieve as for the (H₂O + CO₂) system. A persistence in time dependence was observed which was more significant when the *n*-decane was not purified. The purification step by which polar

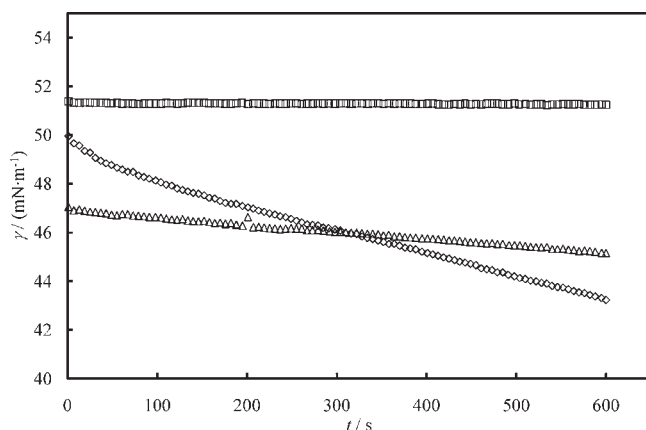


Figure 2. Interfacial tension data of the ($\text{H}_2\text{O} + n\text{-decane}$) system measured using the Wilhelmy plate method, as a function of time for different steps of purification with activated alumina: \diamond , no purification; \triangle , after single, and \square , after triple mixing of $n\text{-decane}$ with fresh activated alumina. The measurements were carried out at ambient conditions: $p = 0.1$ MPa and $T = 295$ K.

impurities (surfactant-like) were removed from the $n\text{-decane}$ was found to be necessary. The difference in time evolution of the interfacial tension of the ($\text{H}_2\text{O} + n\text{-decane}$) system, observed for different steps of mixing the $n\text{-decane}$ with activated alumina prior to measurement, is shown in Figure 2, clearly demonstrating its importance.

RESULTS

The interfacial tension between H_2O and $[(1-x)n\text{-decane} + x\text{CO}_2]$ was investigated for three different compositions of CO_2 in the alkane-rich phase, of mole fractions $x = (0.0, 0.2, \text{ and } 0.5)$, over the temperature range from (298 to 443) K for pressures up to 50 MPa. The values reported, tabulated in Table 2, are the average interfacial tensions and the corresponding standard deviations resulting from a large number of experimental points considered at each state point (≈ 500), out of those collected after the creation of every drop. As for previous systems,^{1,2} a time dependence of interfacial tension was observed, from which the values considered were those between the first and third minutes for the ($\text{H}_2\text{O} + n\text{-decane}$) system, and between the fifth and fifteenth minutes for the two ternary systems, for at least four successive drops at each state point. The reasons for choosing these time regions are discussed below. The interfacial tension data, obtained for different isotherms, can be represented by linear correlations of the form

$$\gamma/(\text{mN}\cdot\text{m}^{-1}) = a(p/\text{MPa}) + b \quad (2)$$

where p is the pressure and a , b are adjustable parameters. The parameters and correlation coefficients are summarized in Table 3.

The time dependence of the interfacial tension for this system had a more significant effect on the determination of a static value than for previous systems studied.^{1,2} This is a common observation as impurities tend to migrate to (aqueous + hydrocarbon) interfaces and so affect, most commonly by reducing, the interfacial tension.^{5,12,13,15} In this case, less time was allowed for the binary system (that did not contain CO_2 as a third component requiring enough time to diffuse into the drop) for acquiring the static interfacial tension values. This follows a similar approach used by Susnar et al.¹⁰ who are the only authors that report dynamic

Table 2. Interfacial Tension Results of the ($\text{H}_2\text{O} + [(1-x)n\text{-Decane} + x\text{CO}_2]$) System^a

| p | T | x | $\Delta\rho$ | γ |
|-------|--------|-----|--------------|------------------|
| | | | | |
| 0.11 | 297.85 | 0.0 | 270 | 51.96 ± 0.28 |
| 0.18 | 323.35 | 0.0 | 281 | 47.78 ± 0.16 |
| 22.25 | 323.35 | 0.0 | 272 | 48.88 ± 0.29 |
| 39.80 | 323.35 | 0.0 | 267 | 49.11 ± 0.25 |
| 0.15 | 343.45 | 0.0 | 286 | 46.28 ± 0.24 |
| 22.85 | 343.45 | 0.0 | 275 | 47.68 ± 0.22 |
| 49.02 | 343.45 | 0.0 | 267 | 48.39 ± 0.21 |
| 0.20 | 374.25 | 0.0 | 291 | 42.87 ± 0.25 |
| 23.00 | 374.25 | 0.0 | 276 | 44.13 ± 0.26 |
| 47.15 | 374.25 | 0.0 | 267 | 45.21 ± 0.72 |
| 0.40 | 403.05 | 0.0 | 292 | 39.59 ± 0.66 |
| 24.50 | 403.05 | 0.0 | 273 | 40.33 ± 0.63 |
| 48.00 | 403.05 | 0.0 | 262 | 40.90 ± 0.59 |
| 1.15 | 442.85 | 0.0 | 288 | 32.36 ± 2.80 |
| 46.40 | 442.85 | 0.0 | 252 | 36.89 ± 0.72 |
| 14.10 | 323.25 | 0.2 | 271 | 39.25 ± 0.36 |
| 21.50 | 323.25 | 0.2 | 267 | 39.19 ± 0.71 |
| 41.60 | 323.25 | 0.2 | 254 | 38.46 ± 0.74 |
| 15.50 | 374.45 | 0.2 | 282 | 36.89 ± 0.42 |
| 27.00 | 374.45 | 0.2 | 274 | 37.43 ± 0.38 |
| 47.00 | 374.45 | 0.2 | 258 | 37.72 ± 0.34 |
| 17.50 | 403.15 | 0.2 | 281 | 33.60 ± 0.51 |
| 25.00 | 403.15 | 0.2 | 275 | 34.40 ± 0.50 |
| 46.00 | 403.15 | 0.2 | 258 | 35.55 ± 0.31 |
| 11.00 | 443.05 | 0.2 | 280 | 28.53 ± 0.50 |
| 22.00 | 443.05 | 0.2 | 272 | 29.75 ± 0.59 |
| 46.00 | 443.05 | 0.2 | 253 | 31.33 ± 1.17 |
| 23.00 | 323.15 | 0.5 | 237 | 34.54 ± 0.49 |
| 33.00 | 323.15 | 0.5 | 230 | 34.76 ± 0.51 |
| 47.00 | 323.15 | 0.5 | 220 | 34.21 ± 0.35 |
| 36.70 | 373.55 | 0.5 | 247 | 31.92 ± 0.50 |
| 46.15 | 373.55 | 0.5 | 237 | 31.54 ± 0.27 |
| 12.60 | 403.15 | 0.5 | 281 | 26.29 ± 1.13 |
| 48.20 | 403.15 | 0.5 | 239 | 29.90 ± 0.57 |
| 14.80 | 443.15 | 0.5 | 284 | 21.72 ± 0.64 |
| 46.00 | 443.15 | 0.5 | 243 | 25.06 ± 0.54 |

^aThe errors correspond to the standard deviation of the interfacial tension data, calculated for all frames recorded between the relevant timeframe after the creation of each drop, for four consecutive drops at each state point. The density difference used for the determination of the interfacial tension at each state point corresponds to that between the density of pure H_2O and pure $n\text{-decane}$ for $x = 0.0$ and that between pure H_2O and the calculated density of the $[(1-x)n\text{-decane} + x\text{CO}_2]$ phase for $x > 0.0$, using SAFT-VR^{22,23} with parameters from previous work.² Standard uncertainties u in pressure and temperature measurement are $u(p) = 5 \cdot 10^{-4} p$ and $u(T) = 0.1$ K, respectively, while the uncertainty in the mole fraction of CO_2 is estimated to be $u(x) = 0.025$, for $x > 0.0$.

interfacial tensions at elevated pressures and temperatures. Most authors report static interfacial tension values (the value of the thermodynamic property at equilibrium). However, the time dependence of interfacial tension makes defining this static condition difficult and appears to be the largest cause for the

Table 3. Parameters for the Linear Correlation of the Interfacial Tension Data for the (H₂O + [(1 - x)n-Decane + xCO₂]) System at Different Isotherms, for the Three Mole Fractions of CO₂ in the n-Decane Phase (cf. Equation 2)

| T/K | a · 10 ³ | b |
|--|---------------------|-------|
| H ₂ O + n-Decane | | |
| 323.35 | 34.22 | 47.88 |
| 343.45 | 42.69 | 46.43 |
| 374.25 | 49.90 | 42.90 |
| 403.05 | 27.59 | 39.60 |
| 442.85 | 100.17 | 32.25 |
| H ₂ O + [0.8 n-Decane + 0.2 CO ₂] | | |
| 323.25 | | 38.97 |
| 374.45 | | 37.34 |
| 403.15 | 65.27 | 32.59 |
| 443.05 | 77.69 | 27.82 |
| H ₂ O + [0.5 n-Decane + 0.5 CO ₂] | | |
| 323.15 | | 34.50 |
| 373.55 | | 31.73 |
| 403.15 | 101.30 | 25.01 |
| 443.15 | 106.98 | 20.14 |

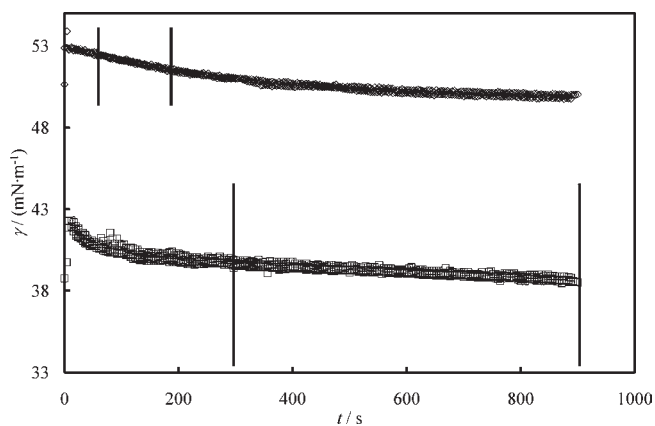


Figure 3. Interfacial tension data of the (H₂O + [n-decane + CO₂]) system measured using the pendant drop method in the high-pressure apparatus, as a function of time for two different conditions: ◇, for the (H₂O + n-decane) system at 297.9 K and 0.11 MPa; and □, for the (H₂O + [0.8 n-decane + 0.2 CO₂]) system at 323.3 K and 14.10 MPa. The vertical lines indicate the ranges over which the values recorded were used for the evaluation of the average interfacial tension, earlier in time for systems without CO₂, and later for systems containing CO₂.

discrepancies between different results reported in the literature. Thus, some consideration of the relevant processes that may affect the measured value is appropriate.

The time dependence of the interfacial tension observed for the (H₂O + [n-decane + CO₂]) system, for the ambient pressure Wilhelmy plate and the high-pressure pendant drop apparatus, is shown in Figures 2 and 3, respectively. In the ambient pressure apparatus, a different number of purification steps employed for the n-decane is compared with respect to the time dependence of the interfacial tension of the (H₂O + n-decane) system. This demonstrated that triple purification of n-decane was necessary

and sufficient, for achieving a substantially time-independent interfacial tension (thus implying no presence of oxidized alkane impurities). The time dependence of the interfacial tension in the high-pressure apparatus, determined for different H₂O drops created in the triply purified n-decane-rich bulk phase, is shown for both ambient conditions (without CO₂) and elevated *p* and *T* (with CO₂) in Figure 3. It is apparent that, for ambient conditions, with the Wilhelmy plate apparatus, the triply purified n-decane demonstrates minimal time dependence of the (H₂O + n-decane) interfacial tension. For the high-pressure pendant drop apparatus, a small, continually reducing trend was observed for the binary (H₂O + n-decane) system, while for systems containing CO₂, a more pronounced initial time dependence was usually found (similar with that observed for the (H₂O + CO₂) system studied previously¹), which stabilized at a quasi-static value, of a slope similar with that of the binary system (see Figure 3). The time dependence of the interfacial tension in the binary system at large times was assumed to be due to the presence of trace amounts of impurities in the high pressure apparatus; thus values of interfacial tension for *t* > 900 s were neglected from the calculation of the average interfacial tension. For the ternary systems, the initial time dependence of the interfacial tension observed was consistent with effects due to diffusion of CO₂ across the H₂O + [n-decane + CO₂] interface.¹ Appropriate time was, therefore, allowed for this to equilibrate, after which the average interfacial tension was obtained. The time range, over which the interfacial tensions recorded were used to calculate the average values, is shown in Figure 3.

The interfacial tension values reported here for the (H₂O + [n-decane + CO₂]) system are those using triply purified n-decane. Initial investigations were also conducted using non triply purified n-decane, which were carried out at the same conditions and compositions as the reported data set. The values in that case were approximately 10 % lower than would be expected from the literature for the binary (H₂O + n-decane) system, which further demonstrated the significance of passing the alkane through activated alumina before measurement. Knowing both from those initial measurements, as well as from the literature, that the interfacial tension pressure dependence for this system is weakly linear, only a few pressure points per isotherm were necessary. This aided in enabling limited exposure and thus minimal aging of the alkane during the study. The results are shown in Figures 4 to 6 for mole fractions of CO₂ in the n-decane phase of *x*_{CO₂} = (0.0, 0.2, and 0.5), respectively.

For the purpose of obtaining the two phase density difference $\Delta\rho$, which is necessary for the calculation of the interfacial tension (see eq 1), H₂O and n-decane or H₂O and (n-decane + CO₂) were treated as immiscible phases. The densities of pure H₂O and pure n-decane were used for the case of the (H₂O + n-decane) binary system, obtained from the National Institute of Standards and Technology (NIST) Chemistry Webbook.²¹ For the case of the (H₂O + [n-decane + CO₂]) ternary system, the molecular based equation of state called the statistical associating fluid theory of variable range (SAFT-VR)^{22,23} was used to calculate the (n-decane + CO₂) phase density. SAFT-VR has a demonstrated ability of describing bulk fluid properties of such mixtures.^{24–26} H₂O was again treated as a pure phase. The relevant SAFT-VR model parameters used were those from our previous work on (n-alkane + CO₂) systems.² The values of interfacial tension obtained from drop shape analysis are linearly dependent on the density difference of the two fluids (see eq 1).

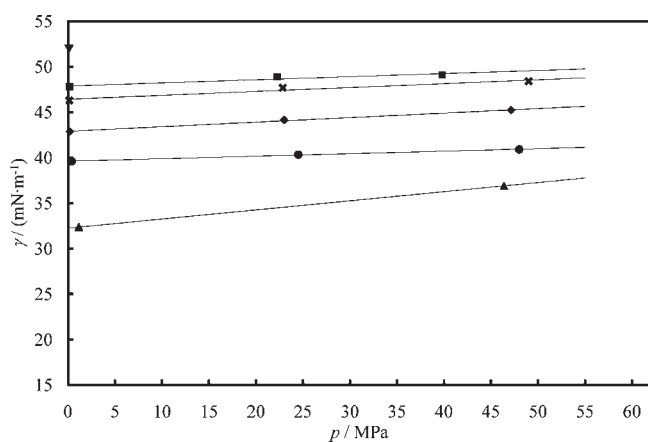


Figure 4. Interfacial tension data of the ($\text{H}_2\text{O} + n\text{-decane}$) system as a function of pressure at different isotherms: ∇ , at 297.9 K; \blacksquare , at 323.4 K; \times , at 343.5 K; \blacklozenge , at 374.5 K; \bullet , at 403.1 K; and \blacktriangle , at 442.9 K.

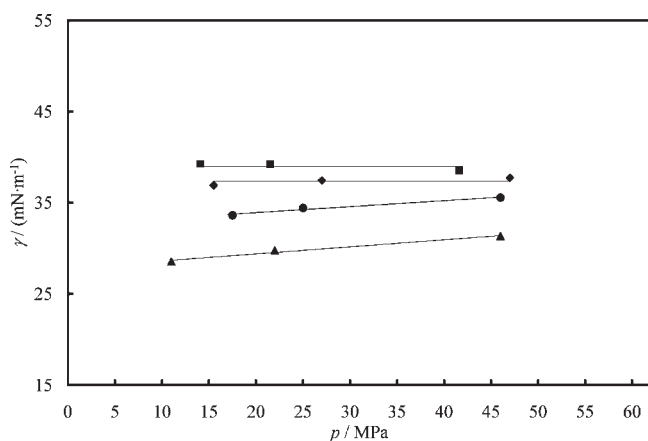


Figure 5. Interfacial tension data of the ($\text{H}_2\text{O} + [0.8 n\text{-decane} + 0.2 \text{CO}_2]$) system as a function of pressure at different isotherms: \blacksquare , at 323.3 K; \blacklozenge , at 374.5 K; \bullet , at 403.2 K; and \blacktriangle , at 443.1 K.

The values of density difference used for the calculation of the interfacial tension are reported in Table 2, allowing for future corrections. If measurements or models reveal that the density difference is significantly different from the values used, then the values of interfacial tension reported here may be corrected by multiplying with the ratio of the new density difference to the one used in the present work.

DISCUSSION

A comparison between the interfacial tension literature values for the binary ($\text{H}_2\text{O} + n\text{-decane}$) system with those obtained in the present work is shown in Figures 7 and 8 for temperature ranges from (298 to 353) K and (353 to 473) K, respectively. At ambient temperature good agreement is seen between the present work and Cai et al.,¹¹ Susnar et al.,¹⁰ and Wiegand and Franck,⁹ while Jennings⁷ and especially Michaels and Hauser,⁵ report significantly lower values (-10%). At higher temperatures, the values of Wiegand and Franck,⁹ Jennings,⁷ and Michaels and Hauser⁵ persist in being lower than those of the present work; Cai et al.¹¹ and Susnar et al.¹⁰ did not investigate higher temperatures. There are no data reported in the literature for the

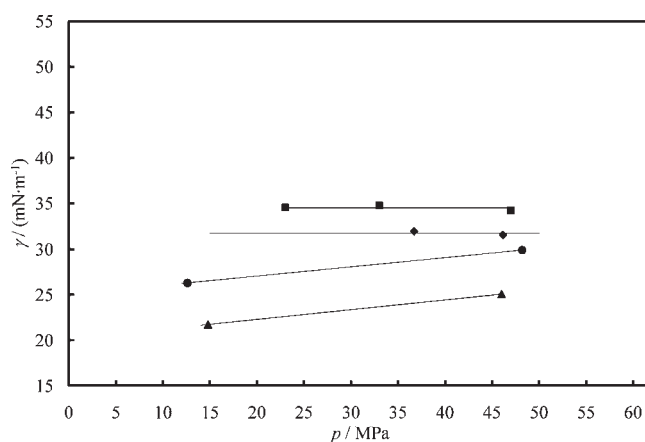


Figure 6. Interfacial tension data of the ($\text{H}_2\text{O} + [0.5 n\text{-decane} + 0.5 \text{CO}_2]$) system as a function of pressure at different isotherms: \blacksquare , at 323.2 K; \blacklozenge , at 373.6 K; \bullet , at 403.2 K; and \blacktriangle , at 443.2 K.

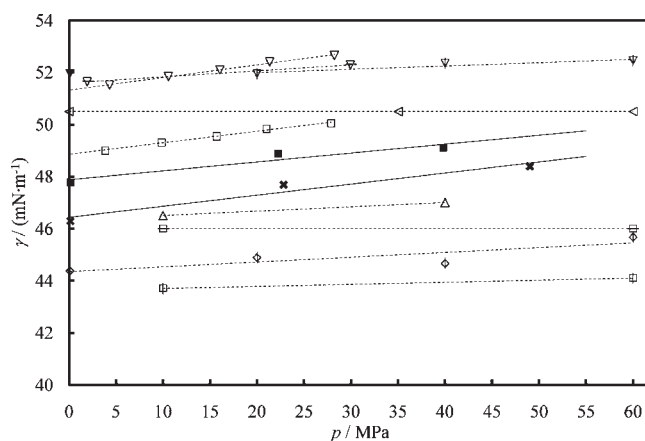


Figure 7. Interfacial tension data of the ($\text{H}_2\text{O} + n\text{-decane}$) system compared to literature values: present work, ∇ , at 297.9 K; \blacksquare , at 323.4 K; and \times , at 343.5 K; and literature values from Cai et al.,¹¹ ∇ , at 298.0 K, and \square , at 323.2 K; Susnar et al.,¹⁰ ∇ with horizontal bar, at 294.7 K; Wiegand and Franck⁹ ∇ with vertical bar, at 295.0 K, and \diamond with vertical bar, at 353.0 K; Jennings⁷ \triangleleft , at 298.2 K; and Michaels and Hauser⁵ \triangle , at 296.70 K, \square with horizontal bar, at 323.3 K, and \square with vertical bar, at 354.1 K. For Michaels and Hauser⁵ and Jennings,⁷ the data points were inferred from graphs.

($\text{H}_2\text{O} + [n\text{-decane} + \text{CO}_2]$) ternary system. The values reported here are the first measurements of interfacial tension for this system.

The obtained data can be plotted against the natural logarithm of the global concentration of the third component (CO_2), demonstrating a decrease of interfacial tension with increasing CO_2 concentration. This is shown in Figure 9, where the interfacial tension is plotted for $p = 60$ MPa as a function of CO_2 composition; isobar values are calculated from the fitting equations and parameters shown in Table 3. The decrease of interfacial tension with increasing concentration of CO_2 suggests that preferential adsorption of CO_2 at the ($\text{H}_2\text{O} + n\text{-decane}$) interface occurs. The Gibbs surface excess concentration, Γ , of CO_2 was calculated for the ($\text{H}_2\text{O} + [n\text{-decane} + \text{CO}_2]$) system, which is given by the relation^{27,28}

$$\Gamma = -\frac{1}{RT} \frac{d\gamma}{d \ln(\alpha_{\text{CO}_2})} \quad (3)$$

Table 4. Fitting Parameters of the Interfacial Tension Data for the (H₂O + [*n*-Decane + CO₂]) System as a Function of Increasing CO₂ Concentration at Different Temperatures (See eqs 3 and 4) for $p = 60$ MPa (by Extrapolation)

| T | $d\gamma/d \ln C$ | $\Gamma_m \cdot 10^{-6}$ | A_{molecule} |
|-----|--------------------|--------------------------|-----------------------|
| K | mN·m ⁻¹ | mol·m ⁻² | nm ² |
| 323 | -3.347 | 1.25 | 75.0 |
| 374 | -4.207 | 1.35 | 81.4 |
| 403 | -4.059 | 1.21 | 73.0 |
| 443 | -4.440 | 1.21 | 72.6 |

Table 5. Fitting Parameters of the Interfacial Tension Data for the (H₂O + [*n*-Decane + CO₂]) System as a Function of Increasing CO₂ Concentration (see Szyszkowski eq 4), at Different Temperatures for $p = 60$ MPa (by Extrapolation), as well as the Calculated ΔG_{ads}^0 from eq 5^a

| T | A | K_{ad} | γ_0 | σ | ΔG_{ads}^0 |
|-----|-----------------------------------|---------------------|--------------------|----------|---------------------------|
| K | m ² ·mol ⁻¹ | L·mol ⁻¹ | mN·m ⁻¹ | | kJ·mol ⁻¹ |
| 323 | 803 137.096 | 15.398 | 49.93 | 0.10 | -7.35 |
| 374 | 739 634.535 | 4.197 | 45.90 | 0.20 | -4.46 |
| 403 | 825 489.120 | 1.585 | 41.26 | 0.46 | -1.54 |
| 443 | 829 289.720 | 1.846 | 38.26 | 0.44 | -2.26 |

^aThe standard error σ is that between the measured values and the fitted Szyszkowski equation, calculated using $\sigma^2 = \sum(\gamma_i - \gamma_s)^2 / (j - n)$, where γ_i is the measured interfacial tension at each state point, γ_s the corresponding fitted interfacial tension using the Szyszkowski equation, j the number of state points, and n the number of fitting parameters.

where $R = 8.314 \cdot 10^3$ mJ·mol⁻¹·K⁻¹ is the gas constant and α_{CO_2} , the activity of CO₂, is taken here as equal to the value of its bulk concentration, C_{CO_2} , assuming an activity coefficient of unity. The slopes $d\gamma/d \ln C$, obtained from the experimental interfacial tension values of the (H₂O + [*n*-decane + CO₂]) system at different isotherms, gave the maximum surface excess CO₂ concentrations, Γ_m . These values, along with the area per CO₂ molecule occupied at the interface ($A = 1/\Gamma_m$), are summarized in Table 4. The surface area A per molecule of CO₂ in this case is found to be in the range (73 to 81) nm², which is more than 2 orders of magnitude greater than the size of the molecule, indicating rather loose adsorption of CO₂ molecules at the interface.

For the calculation of the Gibbs free energy of adsorption, ΔG_{ads}^0 , the Szyszkowski equation,²⁹ based on the Langmuir adsorption isotherm,²⁷ was first fitted to the measured interfacial tension values. The Szyszkowski equation is given by the form

$$\gamma = \gamma_0 - \frac{RT}{A} \ln(1 + K_{\text{ad}} C_{\text{CO}_2}) \quad (4)$$

where $A = 1/\Gamma$ in units of m²·mol⁻¹ is the molar surface area occupied by CO₂ and K_{ad} is its adsorption constant. The interfacial tension is plotted, for various isotherms, as a function of the natural logarithm of CO₂ concentration at $p = 60$ MPa in Figure 9, using values of γ obtained from the fitting equations of interfacial tension as a function of pressure—see Table 3. The continuous curves, shown in Figure 9, correspond to the Szyszkowski equation (eq 4), with K_{ad} as the fitting parameter.

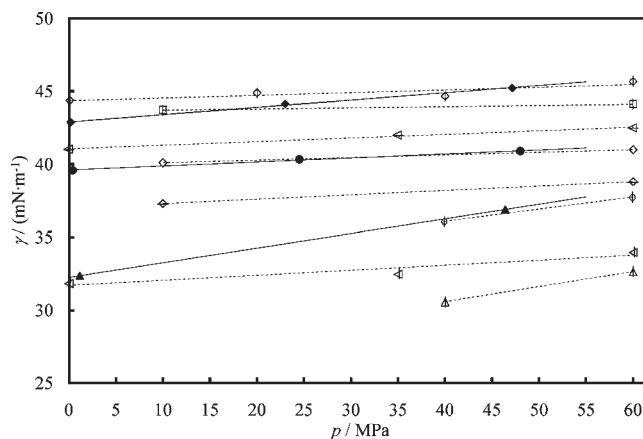


Figure 8. Interfacial tension data of the (H₂O + *n*-decane) system compared to literature values: present work, \blacklozenge , at 374.5 K; \bullet , at 403.1 K, and \blacktriangle , at 442.9 K; and literature values from Wiegand and Franck⁹ \diamond with vertical bar at 353.0 K; \circ with vertical bar at 423.0 K; and \triangle with vertical bar, at 473.0 K; Jennings⁷ \triangleleft with vertical bar at 373.2 K, and \triangleleft with horizontal bar at 449.2 K; and Michaels and Hauser⁵ \square with vertical bar at 354.1 K; \diamond , at 383.9 K; and \diamond with horizontal bar, at 404.9 K. For Michaels and Hauser⁵ and Jennings,⁷ the data points were inferred from graphs.

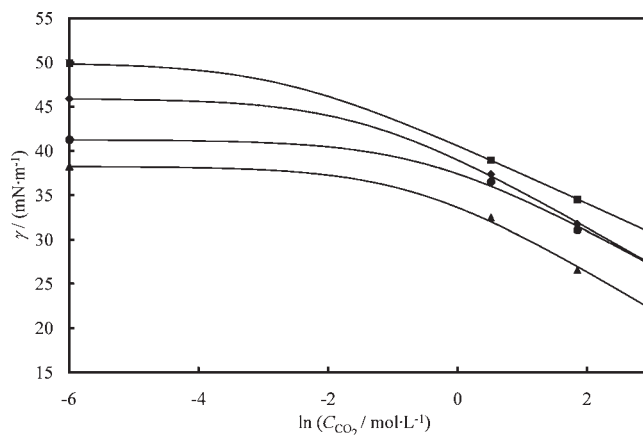


Figure 9. Interfacial tension data of the (H₂O + [*n*-decane + CO₂]) system as a function of the natural logarithm of the concentration of CO₂ at $p = 60$ MPa for different isotherms: \blacksquare , at 323.4 K; \blacklozenge , at 374.5 K; \bullet , at 403.1 K; and \blacktriangle , at 442.9 K. Interfacial tension points at the lowest concentration correspond to the values for the binary (H₂O + *n*-decane) system. Continuous curves correspond to the fitted Szyszkowski equation.

It can be seen that the equation is indeed a good representation of the decrease in interfacial tension from the limiting value γ_0 of the binary (H₂O + *n*-decane) system, as the concentration of CO₂ is increased in the ternary system. It is seen that different isotherms are shifted closer together, as the temperature dependence becomes less significant for higher pressures (also observed in Figures 4 to 6). The Szyszkowski equation has usually been applied in the literature to the adsorption of surfactant molecules at interfaces. It can, however, be applied to the present system as well, in the light of its ability to represent the acquired interfacial tension values as a function of CO₂ concentration.

The values obtained for the molar surface areas, adsorption constants, and fitting errors for the Szyszkowski equation to the

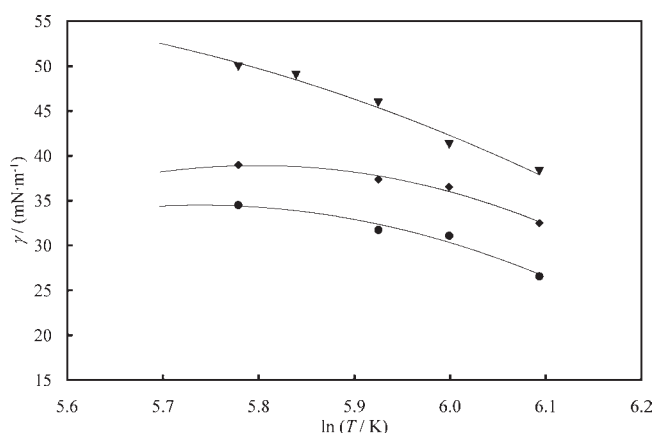


Figure 10. Interfacial tension data of the $(\text{H}_2\text{O} + [(1-x)n\text{-decane} + x\text{CO}_2])$ system as a function of the natural logarithm of temperature at $p = 60$ MPa for different CO_2 mole fractions in the n -decane phase: \blacktriangledown , at $x = 0.0$; \blacklozenge , at $x = 0.2$; and \bullet , at $x = 0.5$.

interfacial tension data are given in Table 5. Using the fitted adsorption constant K_{ad} , the Gibbs free energy of adsorption ΔG_{ads}^0 for CO_2 can be calculated by

$$\Delta G_{\text{ads}}^0 = -RT \ln K_{\text{ad}} \quad (5)$$

the values of which are also listed in Table 5.

The temperature dependence of the interfacial tension at constant pressure can be directly related to the enthalpy of interface formation. The relationship can be quantified through the thermodynamic expression of interfacial tension at constant pressure,³⁰ as

$$-d\gamma/dT = \Delta H^A/T (= \Delta S^A) \quad (6)$$

where ΔH^A is the enthalpy per unit area of interface formation. From eq 6, the relation between ΔH^A and the temperature dependence of interfacial tension becomes

$$-d\gamma/d\ln(T) = \Delta H^A \quad (7)$$

The interfacial tension, measured for the three different compositions of CO_2 in the $(\text{H}_2\text{O} + [n\text{-decane} + \text{CO}_2])$ system, is plotted in Figure 10 against the natural logarithm of temperature at $p = 60$ MPa (again using values obtained from the fitting equations of the interfacial tension as function of pressure—see Table 3). It is observed that for the binary system (no CO_2 addition) the interfacial tension does indeed have a log-linear temperature dependence at this pressure. A similar behavior was also observed at ambient pressure. In the case of the two ternary systems, however, the interfacial tension is less dependent on temperature at ambient conditions, while it decreases at elevated temperatures with a slope similar to that of the binary system, as seen in Figure 10.

The data were fitted for the different compositions of CO_2 by using a quadratic relation of the form

$$\gamma/(\text{mN} \cdot \text{m}^{-1}) = a \ln(T/\text{K})^2 + b \ln(T/\text{K}) + c \quad (8)$$

where a , b , and c are fitted parameters. The mean enthalpy of interface formation was estimated from the results by using eq 8 to obtain the mean slope of the $\gamma-\ln(T)$ plot at each temperature. These are tabulated in Table 6, along with the respective fitting parameters and the standard errors.

Table 6. Fitting Parameters of the Interfacial Tension Data for the $(\text{H}_2\text{O} + [(1-x)n\text{-Decane} + x\text{CO}_2])$ System as a Function of Increasing Temperature (See eqs 8 and 6), for Different CO_2 Mole Fractions in the n -Decane Phase, at $p = 60$ MPa (by Extrapolation)^a

| x | a | $b \cdot 10^3$ | $c \cdot 10^3$ | σ | ΔH^A |
|-----|--------|----------------|----------------|----------|--|
| | | | | | $\text{mJ} \cdot \text{m}^{-2}$ |
| 0.0 | -33.24 | 0.355 | -0.891 | 0.81 | 39.6 |
| 0.2 | -73.18 | 0.848 | -2.422 | 0.39 | $0 < \Delta H^A < 29$ ($\bar{L}^A = 19$) |
| 0.5 | -61.13 | 0.701 | -1.978 | 0.59 | $0 < \Delta H^A < 32$ ($\bar{L}^A = 24$) |

^a The standard error σ is that between the measured values and the fitted quadratic equation, calculated using $\sigma^2 = \sum(\gamma_i - \gamma_f)^2 / (j - n)$, where γ_i is the measured interfacial tension at each state point, γ_f the corresponding fitted interfacial tension using eq 8, j the number of state points, and n the number of fitting parameters.

For the binary $(\text{H}_2\text{O} + n\text{-decane})$ system, a similar analysis at ambient pressure gave a value for the enthalpy of interface formation, $\Delta H^A = 46.9 \text{ mJ} \cdot \text{m}^{-2}$. Comparing this with the value at $p = 60$ MPa, $\Delta H^A = 39.6 \text{ mJ} \cdot \text{m}^{-2}$ indicates that the enthalpy reduces with increasing pressure. Michaels and Hauser⁵ and Jennings⁷ reported average enthalpies of interface formation for the binary $(\text{H}_2\text{O} + n\text{-decane})$ system at pressures up to 60 MPa of $23 \text{ mJ} \cdot \text{m}^{-2}$ and $38 \text{ mJ} \cdot \text{m}^{-2}$, respectively. These values are somewhat consistent with the enthalpies (46.9 and 39.6) $\text{mJ} \cdot \text{m}^{-2}$ found in this work over a similar pressure range. For the systems containing CO_2 , the enthalpy of interface formation is a function of temperature, with values ranging from $(0$ to $32) \text{ mJ} \cdot \text{m}^{-2}$. Table 6 shows that at $p = 60$ MPa the lowest enthalpy is for $x = 0.2$. The significance of the enthalpy of interface formation, the heat required for the interface to maintain its temperature per increased unit area, is that when added to the interfacial tension, it results in the total energy required for the formation of a unit interface. Thus, although the tension may be smaller at one particular state point than at another, because of the different pressure and temperature dependence of ΔH^A , the total energy required for the formation of interfacial area may demonstrate a different relation between the same two state points.

CONCLUSIONS

Interfacial tension measurements have been carried out for the $(\text{H}_2\text{O} + [n\text{-decane} + \text{CO}_2])$ system at different CO_2 compositions for isotherms up to 443 K and pressures up to $p = 50$ MPa. Reasonable agreement with previous literature values was found at ambient pressure for the binary $(\text{H}_2\text{O} + n\text{-decane})$ system, while for higher pressures values in the literature were usually lower than those of the present work. Reasons for these differences are associated with effects from the likely presence of impurities either in high pressure systems or from the chemical compounds used, which can act as surfactants and reduce the interfacial tension. No previous literature values for this ternary system are available.

The data were fitted as a function of pressure by linear correlations, while data on the same isobars were used to demonstrate the relations among the interfacial tension, temperature, and CO_2 composition. These were fitted to correlating equations to within $\pm 2\%$ and were used to derive excess thermodynamic properties for the ternary system, such as surface excess concentrations and Gibbs free energies of adsorption, as well as the

enthalpy of interface formation. The analysis employed for the calculation of the excess properties is usually applied to surfactant systems at ambient conditions; however, it proved to be equally suitable to represent the interfacial tensions of the present system.

The findings of this work have both quantitative and qualitative implications for the deployment of CO₂ in subsurface reservoir processes. The fact that the interfacial tension of the (H₂O + [*n*-decane + CO₂]) system increases with increasing hydrocarbon content and is always larger than that of the binary (H₂O + CO₂) system (see Georgiadis et al.¹) indicates that carbon storage should not be negatively affected by the presence of residual hydrocarbon phases in a storage site. In the context of enhanced oil recovery processes, the extent to which the interfacial tension of the (H₂O + [*n*-decane + CO₂]) system is reduced by increasing the concentration of CO₂ readily links to the decrease of the capillary pressure resisting hydrocarbon displacement through a porous medium when injection of an aqueous phase is applied. Moreover, as *n*-alkane and CO₂ become miscible at elevated pressures and temperatures, as reflected by the vanishing interfacial tensions observed in the (*n*-alkane + CO₂) systems (see Georgiadis et al.²), a combined fluid with improved flow properties is obtained, which further aids the recovery of less mobile, high-viscous hydrocarbons. These two combined effects for the ternary system are of specific interest for water-alternating-gas (WAG) injection schemes, involving the injection of both aqueous and CO₂ phases, where interfacial properties are particularly relevant.

AUTHOR INFORMATION

Corresponding Author

*E-mail: a.bismarck@imperial.ac.uk.

Funding Sources

This work was carried out as part of the Imperial College—Shell Grand Challenge Programme on Clean Fossil Fuels. The authors gratefully acknowledge Shell International Exploration and Production B.V. for supporting the present project and for permission to publish this research. We also acknowledge the support of the Royal Society for a small research grant, which allowed the purchase of the high pressure apparatus.

REFERENCES

- (1) Georgiadis, A.; Maitland, G. C.; Trusler, J. P. M.; Bismarck, A. Interfacial Tension Measurements of the (H₂O + CO₂) System at Elevated Pressures and Temperatures. *J. Chem. Eng. Data* **2010**, *55*, 4168–4175.
- (2) Georgiadis, A.; Llovel, F.; Bismarck, A.; Blas, F. J.; Galindo, A.; Maitland, G. C.; Trusler, J. P. M.; Jackson, G. Interfacial Tension Measurements and Modelling of (Carbon Dioxide + *n*-Alkane) and (Carbon Dioxide + Water) Binary Mixtures at Elevated Pressures and Temperatures. *J. Supercrit. Fluids* **2010**, *55*, 743–754.
- (3) IPCC. *Special Report on Carbon Dioxide Capture and Storage*; Cambridge University Press: Cambridge, U.K., 2005.
- (4) Gibbins, J.; Chalmers, H. Carbon Capture and Storage. *Energy Policy* **2008**, *36*, 4317–4322.
- (5) Michaels, A. S.; Hauser, E. A. Interfacial Tension at Elevated Pressure and Temperature. II Interfacial Properties of Hydrocarbon–Water Systems. *J. Phys. Colloid Chem.* **1951**, *55*, 408–421.
- (6) Harvey, R. R. The Effect of Pressure on the Interfacial Tension of the Benzene–Water System. *J. Phys. Chem.* **1958**, *62*, 322–324.
- (7) Jennings, H. The Effect of Temperature and Pressure on the Interfacial Tension of Benzene–Water and Normal Decane–Water. *J. Colloid Interface Sci.* **1967**, *24*, 323–329.
- (8) Jennings, H.; Newman, G. The Effect of Temperature and Pressure on the Interfacial Tension of Water Against Methane–Normal Decane Mixtures. *SPE J.* **1971**, *11*, 171–175.
- (9) Wiegand, G.; Franck, E. U. Interfacial Tension Between Water and Non-Polar Fluids up to 473 K and 2800 bar. *Ber. Bunsenges. Phys. Chem.* **1994**, *98*, 809–817.
- (10) Susnar, S. S.; Hamza, H. A.; Neumann, A. W. Pressure Dependence of Interfacial Tension of Hydrocarbon–Water Systems Using Axisymmetric Drop Shape Analysis. *Colloids Surf., A* **1994**, *89*, 169–180.
- (11) Cai, B. Y.; Yang, J. T.; Guo, T. M. Interfacial Tension of Hydrocarbon + Water/Brine Systems under High Pressure. *J. Chem. Eng. Data* **1996**, *41*, 493–496.
- (12) Goebel, A.; Lunkenheimer, K. Interfacial Tension of the Water/*n*-Alkane Interface. *Langmuir* **1997**, *13*, 369–372.
- (13) Zeppieri, S.; Rodriguez, J.; de Ramos, A. L. L. Interfacial Tension of Alkane + Water Systems. *J. Chem. Eng. Data* **2001**, *46*, 1086–1088.
- (14) Horozov, T. S.; Binks, B. P.; Aveyard, R.; Clint, J. H. Effect of Particle Hydrophobicity on the Formation and Collapse of Fumed Silica Particle Monolayers at the Oil–Water Interface. *Colloids Surf., A* **2006**, *282*, 377–386.
- (15) Aveyard, R.; Haydon, D. A. Thermodynamic Properties of Aliphatic Hydrocarbon/Water Interfaces. *Trans. Faraday Soc.* **1965**, *61*, 2255–2261.
- (16) Aveyard, R.; Binks, B. P.; Mead, J. Interfacial Tension Minima in Oil–Water–Surfactant Systems. Effects Alkane Chain Length and Presence of *n*-Alkanols in Systems Containing Aerosol OT. *J. Chem. Soc., Faraday Trans. 1* **1986**, *82*, 1755–1770.
- (17) Aveyard, R. Solid–Liquid Dispersions, Vol. 81 of Surfactant Science Series. In *Adsorption of Surfactants at the Solid/Liquid Interface*; Marcel Dekker: New York, 1999; pp 111–130.
- (18) Andreas, J. M.; Hauser, E. A.; Tucker, W. B. Boundary Tension by Pendant Drops. *J. Phys. Chem.* **1938**, *42*, 1001–1019.
- (19) Cheng, P.; Li, D.; Boruvka, L.; Rotenberg, Y.; Neumann, A. W. Automation of Axisymmetric Drop Shape Analysis for Measurements of Interfacial Tensions and Contact Angles. *Colloids Surf.* **1990**, *43*, 151–167.
- (20) Bahramian, A.; Danesh, A.; Gozalpour, F.; Tohidi, B.; Todd, A. C. Vapour–Liquid Interfacial Tension of Water and Hydrocarbon Mixture at High Pressure and High Temperature Conditions. *Fluid Phase Equilib.* **2007**, *252*, 66.
- (21) *Chemistry WebBook*, Standard Reference Database Number 69; National Institute of Standards and Technology: Gaithersburg, MD, 2008.
- (22) Gil-Villegas, A.; Galindo, A.; Whitehead, P. J.; Mills, S. J.; Jackson, G.; Burgess, A. N. Statistical associating fluid theory for chain molecules with attractive potentials of variable range. *J. Chem. Phys.* **1997**, *106*, 4168–4186.
- (23) Galindo, A.; Davies, L. A.; Gil-Villegas, A.; Jackson, G. The thermodynamics of mixtures and the corresponding mixing rules in the SAFT-VR approach for potentials of variable range. *Mol. Phys.* **1998**, *93*, 241–252.
- (24) Galindo, A.; Blas, F. J. Theoretical examination of the global fluid phase behaviour and critical phenomena in carbon dioxide + *n*-alkane binary mixtures. *J. Phys. Chem. B* **2002**, *106*, 4503–4515.
- (25) Blas, F. J.; Galindo, A. Study of the high pressure phase behaviour of CO₂ + *n*-alkane mixtures using the SAFT-VR approach with transferable parameters. *Fluid Phase Equilib.* **2002**, *194–197*, 501–509.
- (26) Colina, C. M.; Gubbins, K. E. Vapor-liquid and vapor-liquid-liquid equilibria of carbon dioxide/*n*-perfluoroalkane/*n*-alkane ternary mixtures. *J. Phys. Chem. B* **2005**, *109*, 2899–2910.
- (27) Adamson, A. W.; Gast, A. P. *Physical Chemistry of Surfaces*, 6th ed.; Wiley: New York, 1997.
- (28) Aveyard, R.; Haydon, D. A. *An Introduction to the Principles of Surface Chemistry*; Cambridge University Press: Cambridge, U.K., 1973.
- (29) Rosen, M. J. *Surfactants and Interfacial Phenomena*, 3rd ed.; Wiley-Interscience: New York, 2004.
- (30) Adam, N. K. *The Physics and Chemistry of Surfaces*, 3rd ed.; Oxford University Press: Oxford, 1941.